Simulation of Joint Design on Weldability of Dissimilar Materials: 405 Ferritic Stainless Steel and 705 Zr Alloy by Friction Welding Process

K. Koundinya[1], A. Chennakesava Reddy[2]

Abstract—The current work was aimed to assess three joints, namely vee-joint, square joint and plain joint, used for joining of dissimilar 705 Zr alloy and 405 ferritic stainless steel materials by continuous drive friction welding. Three joints were evaluated for their strength, heat affected zone and metal flow across the weld joints. The vee-joint was found to be better as compared to plain and square joints.

Index Terms—705 Zr alloy, 405 ferritic stainless steel, frictional pressure, Joint, frictional time, rotation speed, friction welding.

1 INTRODUCTION

THe difficulties in the welding of dissimilar metals by fusion welding processes have been a great challenge for engineering, because of different properties such as hardness, strength and coefficient of thermal expansion associated with them. In continuous drive friction welding, one of the workpieces is attached to a motor driven unit while the other is restrained from rotation as showed in Fig.1a. The motor driven workpiece is rotated at a predetermined constant speed. The workpieces to be welded are forced together and then a friction force is applied as shown in Fig.1b. Heat is generated because of friction between the welding surfaces. This is continued for a predetermined time as showed in Fig.1c. The rotating workpiece is halted by the application of a braking force. The friction force is preserved or increased for a predetermined time after the rotation is ceased Fig. 1d. Fig.1 also illustrates the variation of welding speed, friction force and forging force with time during various stages of the friction welding process.

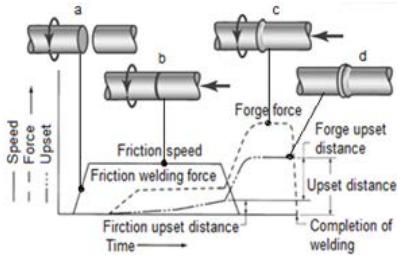

Fig. 1. Friction welding.

With friction welding, joints are possible between not only similar materials, but also dissimilar materials can be welded. The foremost difference between the welding of similar materials and that of dissimilar materials is that the axial movement is unequal in the latter case whilst the similar materials experience equal movement along the common axis. This problem arises not only from the different coefficients of thermal expansion, but also from the distinct hardness values of the dissimilar materials to be joined. The microstructural evolution of the interface of medium carbon steel/austenitic stainless steel depends on thermo-chemical interactions between the two materials [1]. Joint and edge preparation is very important to produce distortion free welds. The solid-state diffusion is slow in the wider joints [2]. The intermetallic compounds can change the micro hardness near the joint interface of dissimilar metals [3]. Therefore, friction welding of dissimilar metals needs to be eased by ensuring that both the workpieces deform similarly. In this context, a research work was carried out with alternative joint designs for the joining interface of mild steel/austenite stainless steel, through a systematic study of incorporating uniform material flow at the interface [4, 5].

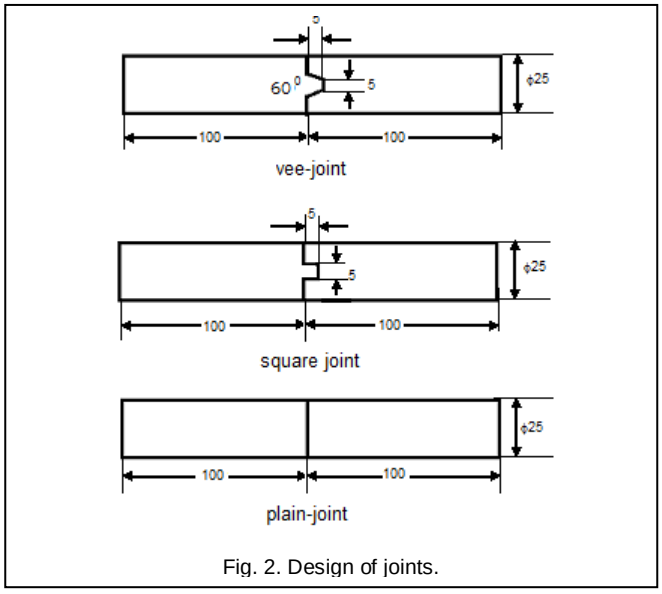

Fig. 2. Design of joints.

Based on the earlier experimental work [4, 5] for various joint designs, the current work was proposed to investigate the per-

- *K. Koundinya is currently pursuing master's degree program in mechanical engineering in JNT University, Hyderabad, India.*
- *A. Chennakesava Reddy is currently working as a Professor in mechanical engineering in JNT University, Hyderabad, India, Ph-9440568776. E-mail: chennakesava@jntuh.ac.in*

formance of friction welding process for dissimilar materials: 705 Zr-alloy and 405 ferritic stainless steel (FSS) using finite element method approach. The designs of three weld joints namely vee joint, square joint and plain joint are shown in figure 2.

2 Materials and Methods

In order to predict the performance of three proposed joints, 705 Zr-alloy and 405 ferritic stainless steel cylindrical bars of 25mm diameter and length of 100mm were considered. The levels chosen for the controllable process parameters are summarized in table 1. Each of the process parameters was chosen at three levels. The orthogonal array (OA), L9 was preferred to carry out experimental and finite element analysis (FEA). The obligation of parameters in the OA matrix is given in table 2.

TABLE 1
CONTROL PARAMETERS AND LEVELS

Factor	Symbol	Level–1	Level–2	Level–3
Frictional pressure, MPa	A	40	45	50
Frictional time, sec	B	4	6	8
Speed, rpm	C	1200	1600	2000
Type of joint	D	Plain	Square	Vee

TABLE 2
ORTHOGONAL ARRAY (L9) AND CONTROL PARAMETERS

Treat No.	A	B	C	D
1	1	1	1	1
2	1	2	2	2
3	1	3	3	3
4	2	1	2	3
5	2	2	3	1
6	2	3	1	2
7	3	1	3	2
8	3	2	1	3
9	3	3	2	1

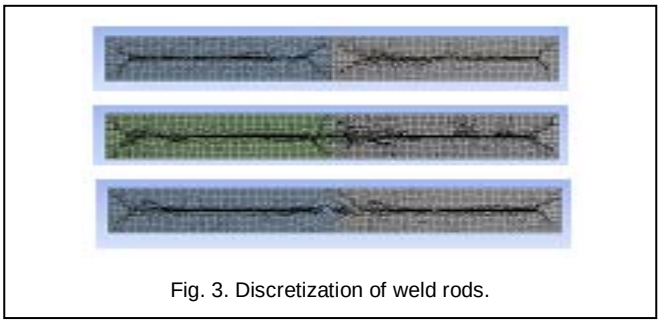

Fig. 3. Discretization of weld rods.

In the finite element analysis of friction welding [6-12], first the transient thermal analysis was performed keeping the 705 Zr alloy rod stationary and the 405 FSS rod in rotation. The coefficient of friction 0.2 was applied at the interface of the 705 Zr alloy and 405 FSS rods. The convection heat transfer coefficient was applied on the surface of two rods. The heat flux calculations were imported from ANSYS APDL commands and applied at the interface of two materials to be welded. The temperature distribution was estimated. The thermal analysis was coupled with the static structural analysis. For the structural analysis the rotating (405 FSS) rod was brought to stationary and the forging pressure was applied on the 705 Zr alloy rod along the longitudinal axis. The 705 Zr alloy rod was allowed to move in the axial direction.

3 Results and Discussion

The statistical Fisher's test was carried out to find the acceptability of process parameters at 90% confidence level.

2.1 Effect of Process Parameters on Temperature

Table – 3 presents the ANOVA (analysis of variation) summary of temperature distribution. The frictional pressure (A), frictional time (B), rotational speed (C) and type of joint (D) would contribute, respectively, 8.40%, 13.57%, 57.71% and 20.31% in the total variation of the welding temperature.

TABLE 3
ANOVA SUMMARY OF TEMPERATURE

Source	Sum 1	Sum 2	Sum 3	SS	v	V	F	P
A	4000.22	3985	4654.5	97302.59	1	97302	162171007	8.4
B	3750.82	4170	4719	157150.67	1	157150	261917821	13.57
C	3265.52	4114	5260.4	668162.16	1	668162	1113603763	57.71
D	3625.72	7722298	12640.32	235090.61	1	235090	391817740	20.31
e				0.0024	4	0.0006	1.00	0
T	14642.28	7734568	27274.22	1157706	8			100

Note: SS is the sum of square, v is the degrees of freedom, V is the variance, F is the Fisher's ratio, P is the percentage of contribution and T is the sum squares due to total variation.

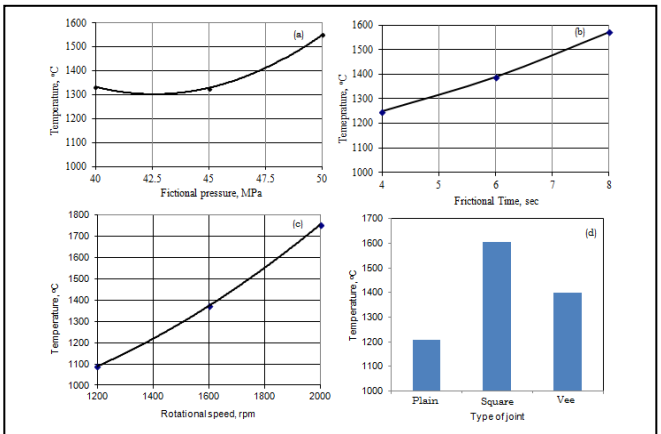

Fig. 4. Effect of process parameters on temperature.

The pressure, frictional time and rotating speed as shown in Fig. 4. The temperature developed in the square joint was higher than that of plain and vee joints. High temperature gradients resulted at the weld interfaces due to high frictional pressure and rotating speed on rods. The welding conditions of trial 3

would generate the highest temperature (1847°C) and trial 1 would produce the lowest temperature (667°C) in the rods (figure 5).

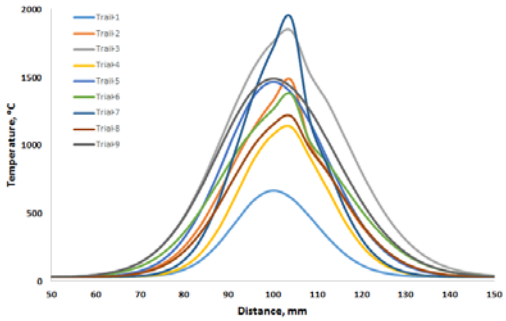

Fig.5. Temperature distribution during different trials.

2.2 Effect of Process Parameters on Effective Stress

The ANOVA summary of the equivalent stress is given in table 4. The contributions were 3.78%, 3.93%, 15.69% and 76.61%, respectively, attributed to frictional pressure (A), frictional time (B), rotational speed (C) and type of joint (D) towards the total variation of effective stress.

TABLE 4
ANOVA SUMMARY OF THE EFFECTIVE STRESS

Source	Sum 1	Sum 2	Sum 3	SS	v	V	F	P
A	1615.45	1709.07	1892.93	13284.93	1	13284	25304615	3.78
B	1591.02	1748	1878.43	13806.58	1	13806	26298233	3.93
C	1473.24	1699	2044.4	55144.44	1	55144	105036974	15.69
D	1442.75	568501	5217.45	269277.12	1	269277	512908533	76.61
e				0.0021	4	0.000525	1.00	0
T	6122.46	573658	11033.21	351513.07	8			100

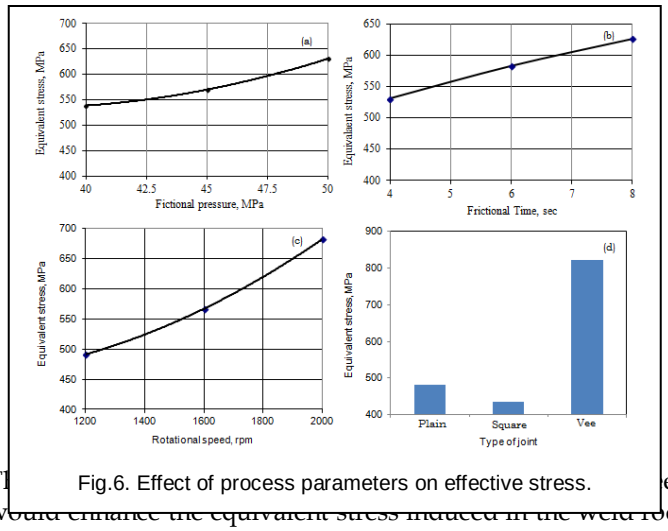

Fig.6. Effect of process parameters on effective stress.

The ... would enhance the equivalent stress induced in the weld rods as shown in Fig. 6. It can also be observed from Fig. 7 that the stress induced in the grain refined region of heat affected zone (HAZ) was higher in all the welds than that in the parent metal. The equivalent stress induced in the vee joint was higher than the rest of the joints. The stress induced in the HAZ for trials 3 and 1 were, respectively, 929.86 MPa and 301.67 MPa as shown in Fig. 8.

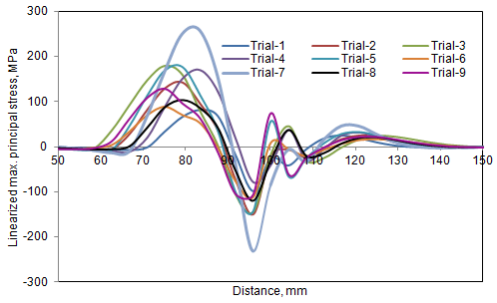

Fig.7. Linearized maximum principle stress in weld rods.

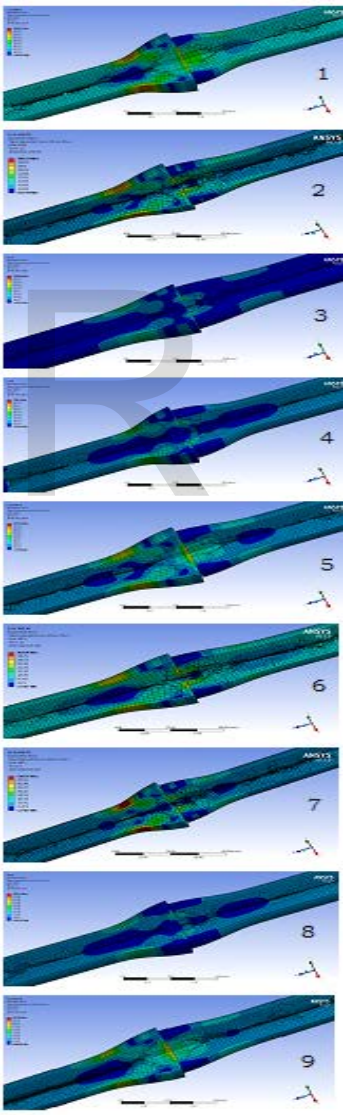

Fig.8. Effect of process parameters on effective stress.

TABLE 5

ANOVA SUMMARY OF THE BULK DEFORMATION

Source	Sum 1	Sum 2	Sum 3	SS	v	V	F	P
A	0.75528	0.71957	0.80314	0	1	0	0.00	0.83
B	0.5154	0.73537	1.02717	0.04	1	0.04	66.43	54.41
C	0.5524	0.74619	0.97939	0.03	1	0.03	49.82	40.6
D	0.73697	0.2	2.277999	0	1	0	0.00	0.83
e				0.0024087	4	0.00060	1.00	3.33
T	2.56014	2.40113	5.087699	0.0724087	8			100

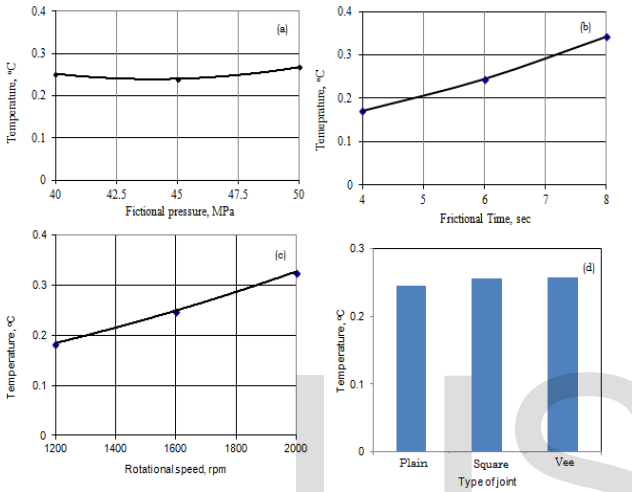

Fig.9. Effect of process parameters on bulk deformation.

2.3 Effect of Process Parameters on Bulk Deformation

The ANOVA summary of the bulk deformation is given in table 5. The major contributions were of frictional time (54.41%), rotational speed (40.60%) and frictional pressure and type of joint (0.83%) towards variation in the bulk deformation. The bulk deformation was found to be minimum for 4 sec of frictional time (Fig. 9b). The effects of frictional pressure and type of joint are nil on the total deformation of the weld rods. The extruded shape was asymmetric, as shown in Fig. 10. The tendency of flange formation was higher with 405 FSS than with 705 Zr alloy. The axial shortening on the 405 FSS side was more than that on 705 Zr alloy side. Consequently, the 405 FSS was moved outward forming the flange at the interface. This is also due to the fact that melting point of 405 FSS is lower than that of 705 Zr alloy.

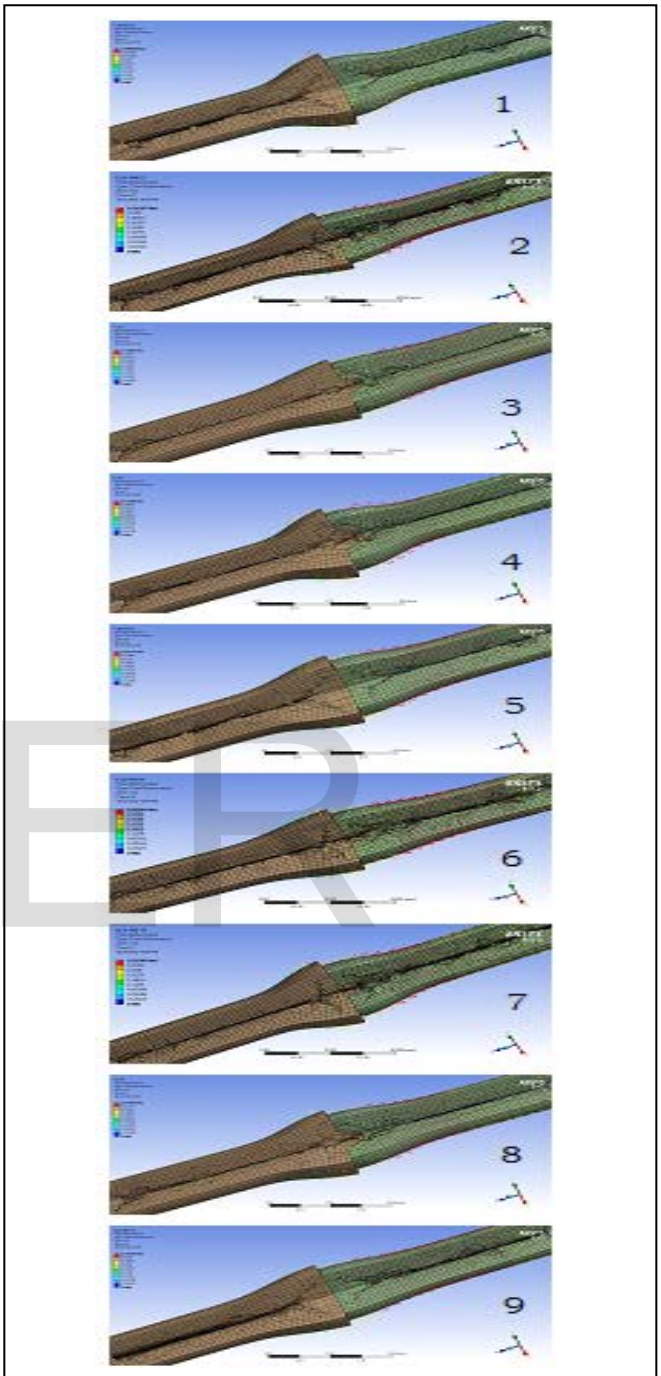

Fig.10. Effect of process parameters on bulk deformation.

4 CONCLUSION

This study shows that the weldability of 705 Zr alloy and 405 ferritic stainless steel is highly dependent on the rotational speed, frictional time and the type of joint. The stresses induced in the vee joint was very high, it is recommended to relieve them using appropriate heat treatment process as the quality of this joint is good. This is because of mechanical interlocking in vee joint and equal bulk deformation with other joints.

ACKNOWLEDGMENT

The authors wish to thank University Grants Commission (UGC), New Delhi for the support of this work.

REFERENCES

[1] M. Sahin, and H.E. Akata, "An experimental study on friction welding of medium carbon and austenitic stainless-steel components",

Industrial Lubrication and Tribology, vol. 56, pp.122-129, 2004.

[2] A. Chennakesava Reddy, A. Ravivarma, and V. Thirupathi Reddy, in Proceedings of National Welding Seminar, IIT-Madras, pp.51-55, 2002.

[3] W. Li and F. Wang, "Modeling of continuous drive friction welding of mild steel", Materials Science and Engineering A, vol. 528, pp.5921-5926, 2011.

[4] A. C. Reddy, "Fatigue Life Evaluation of Joint Designs for Friction Welding of Mild Steel and Austenite Stainless Steel," International Journal of Science and Research, vol. 4, no. 2, pp. 1714-1719, 2015.

[5] A. C. Reddy, "Fatigue Life Prediction of Different Joint Designs for Friction Welding of 1050 Mild Steel and 1050 Aluminum," International Journal of Scientific & Engineering Research, vol. 6, no. 4, pp. 408-412, 2015.

[6] V. Srija and A. C. Reddy, "Finite Element Analysis of Friction Welding Process for 2024Al Alloy and UNS C23000 Brass," International Journal of Science and Research, vol. 4, no. 5, pp. 1685-1690, 2015.

[7] T. Santhosh Kumar and A. C. Reddy, "Finite Element Analysis of Friction Welding Process for 2024Al Alloy and AISI 1021 Steel," International Journal of Science and Research, vol. 4, no. 5, pp. 1679-1684, 2015.

[8] A. Raviteja and A. C. Reddy, "Finite Element Analysis of Friction Welding Process for UNS C23000 Brass and AISI 1021 Steel," International Journal of Science and Research, vol. 4, no. 5, pp. 1691-1696, 2015.

[9] A. C. Reddy, "Finite Element Analysis of Friction Welding Process for AA7020-T6 and Ti-6Al-4V Alloy: Experimental Validation," International Journal of Science and Research, vol. 4, no. 5, pp. 947-952, 2015.

[10] A. C. Reddy, "Evaluation of parametric significance in friction welding process for AA2024 and Zr705 alloy using finite element analysis," International Journal of Engineering Research & Technology, vol. 5, no. 1, pp. 84-89, 2016.

[11] A. Chennakesava Reddy, "Weldability of Friction Welding Process for AA2024 Alloy and SS304 Stainless Steel using Finite Element Analysis," International Journal of Engineering Research and Application, vol. 6, no. 3, pp. 53-57, 2016.

[12] A. Chennakesava Reddy, "Evaluation of Parametric Significance in Friction Welding Process for AA7020 and Zr705 Alloy using Finite Element Analysis," International Journal of Emerging Technology and Advanced Engineering, vol. 6, no. 2, pp. 40-46, 2016.